

香港中文大学 (深圳)  
The Chinese University of Hong Kong, Shenzhen

DDA3005

NUMERICAL METHODS

INSTRUCTOR: DR. ANDRE MILZAREK

---

# Course Project Singular Value Decomposition

---

Group Name: Macrohard

December 27, 2022

## Group Members

ID	Name in Chinese	Name in English	Tasks Involved
120090549	温子雄	WEN Zixiong	2
120090135	王子文	WANG Ziwen	3, Report
120090470	李鹏	LI Peng	1
120090224	杨尚霖	YANG Shanglin	3, Report
120090771	邱纬纶	QIU Weilun	1, 2, 3, Report

## Contents

<b>1</b>	<b>Summary of the Project</b>	<b>2</b>
<b>2</b>	<b>Singular Value Decomposition</b>	<b>2</b>
2.1	About Part 1 . . . . .	2
2.2	Algorithmic Component I - Golub-Kahan bidiagonalization . . . . .	3
2.3	Algorithmic Component II - QR iteration with Wilkinson Shift and Deflation . . . . .	4
2.4	Algorithmic Component III - alternative iterative procedure of QR iteration . . . . .	4
2.5	Main Results and Observation . . . . .	5
<b>3</b>	<b>Deblurring Revisited</b>	<b>5</b>
3.1	About Part II . . . . .	5
3.2	Main Results and Observation . . . . .	6
3.2.1	Quality of Reconstruction in Model I . . . . .	6
3.2.2	Quality of Reconstruction in Model II . . . . .	7
3.2.3	Comparing Performance of QR Iteration and Alternative Iteration . . . . .	8
<b>4</b>	<b>Power Iterations and Video Background Extraction</b>	<b>8</b>
4.1	About Part III . . . . .	8
4.2	Main Results and Observation . . . . .	8
4.3	Comparison between the required time of non-sparse-based power method and sparse-based power method . . . . .	11
4.4	Convergence of power method . . . . .	11
<b>5</b>	<b>Appendix</b>	<b>13</b>
5.1	Appendix-1.1: procedure of QR iteration using Wilkinson Shift and Deflation . . . . .	13
5.2	Appendix-1.2: example of the output in part 1 . . . . .	14
5.3	Appendix-2.1: examples and data obtained when measuring the quality of re- construction in model I . . . . .	15
5.4	Appendix-2.2: examples and data obtained when measuring the quality of re- construction in model II . . . . .	17
5.5	Appendix-2.3: comparing performance of QR iteration with Wilkinson Shift and alternative iteration . . . . .	19
5.6	Appendix-3.1: More background extraction examples . . . . .	20

# 1 Summary of the Project

This is a course project of numerical methods which consists of three parts.

In the first part, we implement a two-phase procedure to perform singular value decomposition on a matrix  $A$ . In phase I, the matrix is first reduced to bidiagonal form via Golub-Kahan bidiagonalization. The resulting bidiagonal matrix  $B$  will be the input of the second phase. In phase II, different iterative procedure is applied to obtain the eigenvectors and eigenvalues of matrix  $B^T B$ . The SVD of  $B$  and  $A$  can then be constructed using these results.

In the second part, we apply SVD to image deblurring problem. The first step is to build two blurring kernels  $A_l \in \mathbb{R}^{n \times n}$  and  $A_r \in \mathbb{R}^{n \times n}$ , where  $n$  is the size of the image. Here, we adopt two different models in the application, which will be discussed in the third section. The blurry image can be constructed using the two kernels. In the second step, the truncation technique is used to generate the pseudoinverse  $A_l^+$  and  $A_r^+$ . The blurry images are deblurred using the truncated reconstruction of pseudoinverses. We calculate peak-signal-to-noise-ratio (PSNR) to measure the quality of reconstruction and compare the runtimes of SVDs using the two iterative procedures mentioned in the first part.

In the third part, we utilize power method with Rayleigh quotient to extract background from a .mp4 video. The first step is to extract  $s$  frames from a video with resolution  $m \times n$  and resize these frames into a matrix  $A \in \mathbb{R}^{mn \times s}$ . The second step is to run power method on  $A^T A$  to obtain  $A$ 's largest singular value  $\sigma$  and corresponding singular vectors  $u$  and  $v$ . The last step is to obtain the background matrix  $\text{vec}(B)$ , which will later be converted into an image, using  $\sigma$ ,  $u$  and  $v$ .

## 2 Singular Value Decomposition

### 2.1 About Part 1

In the first part of the project, we implement the **singular value decomposition (SVD)** of a matrix using a **two-phase procedure**. An SVD of a matrix  $A \in \mathbb{R}^{m \times n}$  factorizes the matrix in the following form.

$$A = U \Sigma V^T \tag{2.1}$$

The matrix  $U$  is generated by stacking eigenvectors of the matrix  $AA^T \in \mathbb{R}^{m \times m}$ . The matrix  $V$  follows a similar custom, which is formed by stacking eigenvectors of the matrix  $A^T A \in \mathbb{R}^{n \times n}$ . The matrix  $\Sigma \in \mathbb{R}^{m \times n}$  contains the information of singular values  $\sigma_i$ ,  $i = 1, 2, \dots, \min\{n, m\}$  at its main diagonal.

The two phases of the procedure is described as following.

- Phase I: Conduct the **Golub-Kahan bidiagonalization** to reduce the matrix  $A$  to bidiagonal form. The resulting matrix is denoted as  $B$ .
- Phase II-A: Perform **QR iteration** with **Wilkinson shift** and **deflation** on matrix  $B^T B$ . The output of this phase will be the eigenvectors and the eigenvalues of  $B^T B$ .

With the above outputs, the SVD of matrix  $B$  can be constructed. The SVD of the original matrix  $A$  can be constructed based on the SVD of  $B$ .

Besides, an alternative method of the QR iteration is adopted in phase II-B, which follows the following scheme.

- Phase II-B: Replace the QR iteration with the following iteration.

$$\begin{aligned} &\text{Initilize } X^0 = B \text{ and for } k = 0, 1, \dots \text{ do:} \\ &Q_k R_k = (X^k)^T, \quad L_k L_k^T = R_k R_k^T, \quad X^{k+1} = L_k^T \end{aligned} \tag{2.2}$$

This iterative procedure is in fact equivalent to the original QR iteration, which will be varified in the following sections.

## 2.2 Algorithmic Component I - Golub-Kahan bidiagonalization

Following the two-phase approach scheme, the first step is to bidiagonalize the matrix in an iterative way. For the bidiagonal matrix constructed in this project, the main diagonal and the diagonal above consist of nonzero entries. Therefore, in each iteration we apply two householder reflections on the left and right. The left one introduces zeros to entries below the diagonal while the right one introduces zeros to the right of the superdiagonal.

$$\begin{aligned} &\text{for } k = 0, 1, \dots, \text{ let } a_k \text{ be the } (k+1)\text{-th column of the matrix and do:} \\ &v_k = a_k \pm \|a_k\|e_k, \quad H v_k = I_k - 2 \frac{v_k v_k^T}{\|v\|_2^2}, \quad A_{k+1} \rightarrow \begin{bmatrix} I_k & \mathbf{0} \\ \mathbf{0} & H v_k \end{bmatrix} \cdot A_k \end{aligned} \tag{2.3}$$

The above scheme shows the procedure of householder transformation on columns. The procedure of row reducing is similar to this scheme except that each row vector  $b_k$  does not

need to include the element in the main diagonal. The general procedure of bidiagonalization is shown as following.

$$\begin{aligned}
 &\text{for } k = 0, 1, \dots, \text{ do:} \\
 &\quad \text{build } U_k^T \text{ using scheme (1.3) on column } k \\
 &\quad \text{build } V_k \text{ using scheme (1.3) on row } k \\
 &\quad A_{k+1} \rightarrow U_k^T A_k V_k
 \end{aligned} \tag{2.4}$$

### 2.3 Algorithmic Component II - QR iteration with Wilkinson Shift and Deflation

The general procedure of the entire algorithm is described by the pseudocode posted in Appendix-1.1. The algorithm takes a square matrix  $A \in \mathbb{R}^{n \times n}$  as input and output a list of eigenvalues  $\lambda_i$ ,  $i = 1, \dots, n$  and a matrix  $Q$  whose columns are the eigenvectors of the corresponding eigenvalues in the list. The Wilkinson shift is computed by calculating the eigenvectors of the  $2 \times 2$  matrix at the lower right corner of the matrix. The shift value will be selected to be the eigenvalues which is closer to the value in the entry  $A(r, r)$ ,  $r = 1, \dots, n$ . As for deflation, the algorithm keeps track of the norm of the vector  $A(1 : r - 1, r)$  and once it is smaller than the preset tolerance, deflation is conducted. In actual implementation, the tolerance is set as  $\text{tol} = 1\text{e-}11$ .

### 2.4 Algorithmic Component III - alternative iterative procedure of QR iteration

In this part, the iterative procedure described in (1.2) is implemented. This procedure actually coincides with the QR iteration with zero shift. The equivalence will be shown as following.

For the  $k$ -th iteration of the QR algorithm, we have that

$$\begin{aligned}
 Q_k R_k &= X^{k-1} \\
 X^k &= R_k Q_k.
 \end{aligned} \tag{2.5}$$

Therefore,  $R_k = Q_k^T X^{k-1}$  and  $X^k = Q_k^T X^{k-1} Q_k$  are satisfied. If this result is applied to all the previous iterations, we have

$$X^k = Q_k^T Q_{k-1}^T \cdots Q_1^T X^0 Q_1 \cdots Q_{k-1} Q_k. \tag{2.6}$$

Therefore, when  $B^T B$  is applied to QR iteration, we have that

$$X^k = Q_k^T Q_{k-1}^T \cdots Q_1^T B^T B Q_1 \cdots Q_{k-1} Q_k \quad (2.7)$$

Similarly, in the  $k$ -th iteration of our alternative method (2.2), we have  $R_k = Q_k^T (X^k)^T$ . Since  $X^{k+1} = L_k^T$  and  $L_k L_k^T = R_k R_k^T$  is satisfied, we have that

$$(X^{k+1})^T X^{k+1} = Q_k^T (X^k)^T X^k Q_k \quad (2.8)$$

Apply the above result to all the previous iterations, and set  $X^0 = B$ , we have

$$(X^{k+1})^T X^{k+1} = Q_k^T Q_{k-1}^T \cdots Q_1^T Q_0^T B^T B Q_0 Q_1 \cdots Q_{k-1} Q_k. \quad (2.9)$$

It turns out that  $(X^{k+1})^T X^{k+1}$  in equation (2.9) is equivalent to  $X^k$  in equation (2.7). The difference is that the diagonal elements of the output  $X^k$  in QR iteration converge to eigenvalues of  $B^T B$ , while in the alternative method, they converge to singular values directly.

## 2.5 Main Results and Observation

An example of the output of the program can be seen in Appendix-1.2. The number of iterations of the alternative iteration is set as 1000. From the results, both methods are able to give reliable results.

# 3 Deblurring Revisited

## 3.1 About Part II

For this part of the project, the SVD program implemented in part 1 is utilized to finish deblurring tasks. In this project, deblurring problems with the following form are considered.

$$B = A_l X A_r \quad (3.1)$$

In the above equation,  $X \in \mathbb{R}^{n \times n}$  represents the matrix of original image. The resulting blurry image will be  $B \in \mathbb{R}^{n \times n}$ . The matrix  $A_l \in \mathbb{R}^{n \times n}$  and  $A_r \in \mathbb{R}^{n \times n}$  are the left and right blurring kernels. To reconstruct the original image from a given blurry image  $B$  and the two blurring kernels, we need to compute the pseudoinverses  $A_l^+$  and  $A_r^+$  and the recovered image can be obtained by  $X = A_l^+ B A_r^+$ .

The first step of this part is to construct the blurring kernels. Two different models are used to blur the images.

- Model I: We set  $A_l = A_r = T^k$  where  $k = 40$  and matrix  $T$  has the following form.

$$T = \begin{bmatrix} \frac{2+\delta}{4+\delta} & \frac{1}{4+\delta} & & & \\ \frac{1}{4+\delta} & \frac{2+\delta}{4+\delta} & \frac{1}{4+\delta} & & \\ & \ddots & \ddots & \ddots & \\ & & \ddots & \ddots & \frac{1}{4+\delta} \\ & & & \frac{1}{4+\delta} & \frac{2+\delta}{4+\delta} \end{bmatrix} \in \mathbb{R}^{n \times n}, \delta = 0.1 \quad (3.2)$$

- Model II: The matrix  $A_l$  and  $A_r$  are both symmetric and have the following form.

$$A = \begin{bmatrix} a_n & a_{n-1} & & a_2 & a_1 \\ a_{n-1} & a_n & a_{n-1} & & a_2 \\ & \ddots & \ddots & \ddots & \\ a_2 & & \ddots & \ddots & a_{n-1} \\ a_1 & a_2 & & a_{n-1} & a_n \end{bmatrix}, \quad \sum_{i=1}^n a_i = 1, \quad a_i \geq 0 \quad (3.3)$$

In this case,  $A_l$  and  $A_r$  are different symmetric matrices and the blurring kernel computes the weighted average of the pixels to generate the blurry image.

To compute the inverse (or pseudoinverse) of  $A_l$  and  $A_r$ , the truncated SVD technique is applied. According to SVD of a matrix  $A$  with rank  $r$ , we have that  $A = U\Sigma V^T = \sum_{i=1}^r \sigma_i u_i v_i^T$ . Therefore, the matrix  $A^+$  can be computed as  $A^+ = V\Sigma^{-1}U^T = \sum_{i=1}^r \frac{1}{\sigma_i} v_i u_i^T$ . With additional parameters  $l_{\text{trunc}}$  and  $r_{\text{trunc}}$ , the two matrices can be constructed as

$$A_{l,\text{trunc}}^+ = \sum_{i=1}^{l_{\text{trunc}}} \frac{v_i^l (u_i^l)^T}{\sigma_i}, \quad A_{r,\text{trunc}}^+ = \sum_{i=1}^{r_{\text{trunc}}} \frac{v_i^r (u_i^r)^T}{\sigma_i} \quad (3.4)$$

## 3.2 Main Results and Observation

### 3.2.1 Quality of Reconstruction in Model I

The quality of the reconstruction is related to the choice of the parameter  $l_{\text{trunc}}$  and  $r_{\text{trunc}}$ .



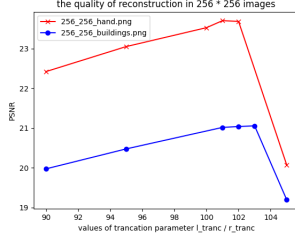


Figure 1: 256 × 256 image

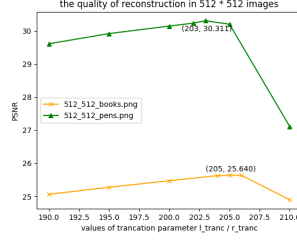


Figure 2: 512 × 512 image

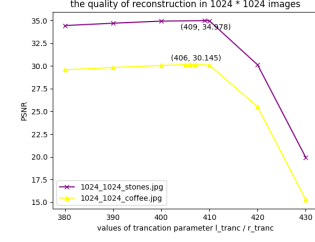


Figure 3: 1024 × 1024 image

The above three figures show the results obtained by applying 6 images to model I with various sizes. An observation of the relation between peak-signal-to-noise ratio (PSNR) and trancation parameters  $l_{\text{trunc}}$  and  $r_{\text{trunc}}$  is that the PSNR increases as the trancation parameters increase when  $l_{\text{trunc}} = r_{\text{trunc}} < l^*$ . When  $l_{\text{trunc}} = r_{\text{trunc}} = l^*$ , the reconstructed image will have the largest PSNR. When the trancation parameters are larger than the optimal value  $l^*$ , the PSNR of the reconstruction sharply decreases. Another observation is that the value of the threshold  $l^*$  depends on the size of the image. From Figure 1, the trancation value which gives the best quality of reconstruction is around 102 (101 for 256\_256\_hand.png and 103 for 256\_256\_buildings.png). As for 512 × 512 images, the optimal value of  $l_{\text{trunc}}$  and  $r_{\text{trunc}}$  is around 203. For 1024 × 1024 images, this value will change to around 406.

### 3.2.2 Quality of Reconstruction in Model II

The experiment on model II presents a result that is different from model I.

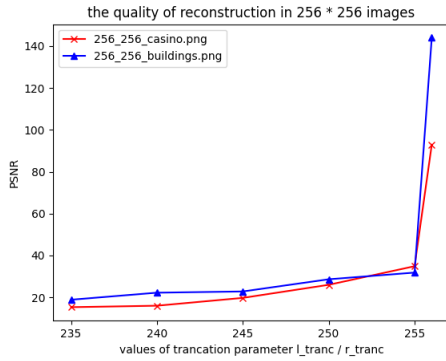


Figure 4: 256 × 256 image

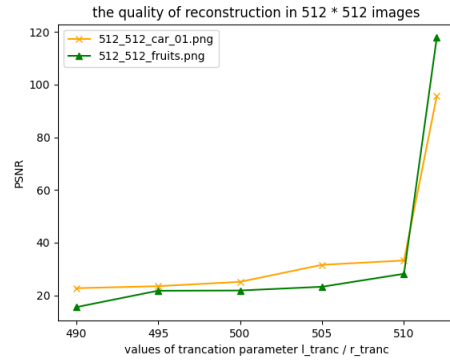


Figure 5: 512 × 512 image

In this case, the PSNR increases as the value of the trancation parameter increases. In

addition, the PSNR increases sharply when the last singular value and singular vectors are applied to construct pseudoinverse. The corresponding data and the effect of deblurring in this model are shown in Appendix-2.2.

### 3.2.3 Comparing Performance of QR Iteration and Alternative Iteration

To compare the performance between the QR iteration and the alternative iteration, we test on 3 different cases. The results are shown in Appendix-2.3. Generally speaking, the two methods reconstruct the figure with almost the same level of quality (similar PSNR). However, the alternative iteration requires a longer run time in general.

## 4 Power Iterations and Video Background Extraction

### 4.1 About Part III

The core goal in this part is to obtain the largest singular value  $\sigma$  and corresponding singular vectors  $u$  and  $v$  for a given matrix  $A \in \mathbb{R}^{mn \times s}$ . After this part is finished,  $\text{vec}(\mathbf{B})$ , i.e., the extracted background, will be obtained.

A brute-force method can be utilizing the built-in SVD to do a complete SVD for  $A$ , and then selecting  $u$ ,  $\sigma$  and  $v$  from this SVD. However, there exist other methods that avoid calculating other singular values and singular vectors.

Power method with Rayleigh quotient can solve this problem efficiently. The first step is to run power method to obtain the largest eigenvalue and corresponding eigenvector of  $A^T A$ . Since  $mn$  is far larger than  $s$ , the largest singular value  $\sigma$  of  $A$  is the square root of the largest eigenvalue  $\lambda$  of  $A^T A$ . The corresponding right singular vector  $v$  is the eigenvector of  $A^T A$  that corresponds to  $\lambda$ . The corresponding left singular vector  $u$  can be obtained by solving

$$Av = \sigma u \tag{4.1}$$

### 4.2 Main Results and Observation

When computing the largest singular value and corresponding singular vectors of a matrix, power method with Rayleigh quotient is about 5 ~ 10 times faster than the built-in SVD. As

shown in Figure 6-11 for pedestrians.mp4, power method only requires about fifty frames and one iteration to extract a clear background.



**Figure 6:** 10 frames, 1 iteration

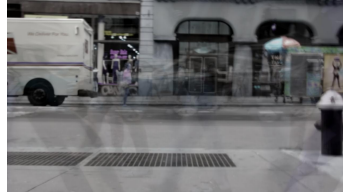


**Figure 7:** 10 frames, 3 iterations

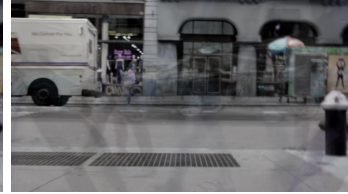


**Figure 8:** 10 frames, 5 iterations



**Figure 9:** 20 frames, 1 iteration



**Figure 10:** 50 frames, 1 iteration



**Figure 11:** 100 frames, 1 iteration

The background quality is mainly restricted by the number of frames. Power method converges so fast that one to three iterations are enough.

Table 1 records the required time of power method when given different resolution of videos, number of frames and maximum number of iterations.

**Table 1:** Performance of power method

Video	# of frames	# of iterations	Time(s)
2560_1440/people_02	100	5	115.29
		3	100.95
		1	88.32
	10	5	4.09
1920_1080/sunset	100	5	33.72
		3	24.62
		1	28.88
	10	5	2.36
1280_720/pedestrians	100	5	9.14
		3	8.96
		1	9.66
	10	5	0.97

The required time of power method grows quickly with higher resolution of video and more frames, but grows slowly with more iterations. It is uncommon that for the two videos with lower resolution, 3 iterations require less time than 1 resolution. One possibly related fact is that under relative low resolution and few iterations, the running time mainly results from converting video into frame matrices, and repeating few more iterations will not be much a burden. However, it is still opaque why running time will decrease from 1 to 3 iterations.

Table 2 compares the performance between power method and built-in SVD.

**Table 2:** Average performance of power method with 5 iterations and built-in SVD

Video	Power method(s)	Built-in SVD(s)
2560_1440/people_02	0.013674	0.072699
1920_1080/sunset	0.003922	0.025831
1280_720/pedestrians	0.001525	0.010016

In Table 2, right two columns record the required time of two implementations to obtain the largest singular value and corresponding singular vectors for each of the 10 frame matrices on average. Power method is about 5 ~ 10 times faster than built-in SVD.

This result can be reproduced by running main.py. More examples are available in

Appendix-3.1.

### 4.3 Comparison between the required time of non-sparse-based power method and sparse-based power method

The power method above uses `scipy.sparse`. Though each frame matrix is very unlikely to be sparse, initially, reporters still speculated that using sparse methods can optimize performance. For verification, reporters also tried a non-sparse design and found it actually faster than the previous sparse-based power method. Table 3 compares their performance in obtaining  $\text{vec}(\mathbf{B})$  out of a random non-sparse matrix  $\mathbf{A} \in \mathbb{R}^{400 \times 300}$ .

**Table 3:** Performance of sparse and non-sparse power method

Sparse(s)	Non-sparse(s)
0.375897	0.034405

In Table 3, average performance is obtained from ten randomly generated  $\mathbf{A} \in \mathbb{R}^{400 \times 300}$ . On average, non-sparse power method is about 10 times faster than sparse. It might be explained by that `scipy.sparse` techniques are slower than non-sparse techniques when the input matrix is dense. It requires an amount of time to convert a common NumPy matrix into a `scipy.sparse` matrix, which dominates the running time when given dense input matrix. Due to limited time, reporters did not update the non-sparse design to the final codes.

This result can be reproduced by running `test_time.py`.

### 4.4 Convergence of power method

Non-sparse and sparse power method obtain the same result after each iteration. Therefore, reporters chose non-sparse power method to test its convergence.

**Table 4:** Convergence of power method

# of iterations	Power method(s)	Built-in SVD(s)	Error of $u$	Error of $\sigma$	Error of $v$
1	0.001093	0.018152	$1.3 \times 10^{-3}$	$6.1 \times 10^{-2}$	$2.6 \times 10^{-2}$
3	0.000997	0.018152	$1.2 \times 10^{-8}$	$3.8 \times 10^{-12}$	$2.1 \times 10^{-7}$
5	0.001198	0.016654	$1.1 \times 10^{-13}$	$2.8 \times 10^{-14}$	$2.0 \times 10^{-12}$
10	0.001287	0.020544	$9.2 \times 10^{-16}$	$5.7 \times 10^{-14}$	$6.6 \times 10^{-15}$
20	0.002895	0.026227	$4.3 \times 10^{-16}$	$2.8 \times 10^{-14}$	$4.2 \times 10^{-15}$

In table 4, the second and third columns record the average time to compute the largest singular value  $\sigma$  and corresponding singular vectors  $u$  and  $v$ . The error of an attribute after some iterations is the Euclidian norm of the difference between its value and the value obtained from built-in SVD. Power method converges to an accuracy of  $10^{-12}$  after 5 iterations. Such an accuracy is enough for background extraction. This fact explains why iterating more does not significantly improve the quality of the background.

This result can be reproduced by running `test_converge.py`.

## 5 Appendix

### 5.1 Appendix-1.1: procedure of QR iteration using Wilkinson Shift and Deflation

```

input:  $A \in \mathbb{R}^{n \times n}$ 
set  $Q = Q_{\text{tmp}} = I_n \in \mathbb{R}^{n \times n}$ 
for  $r = n$  to 2 do:
     $k = 0$ ,  $X^0 = A(1 : r, 1 : r)$ 
    while True:
         $k = k + 1$ 
         $\sigma_{k-1} = \text{Wilkinson\_shift}(X^{k-1})$ 
         $Q_k R_k = X^{k-1} - \sigma_{k-1} I$ 
         $X^k = R_k Q_k + \sigma_{k-1} I$ 
         $Q_{\text{tmp}} = Q_{\text{tmp}} \cdot Q_k$ 
        if  $X^k(1 : r - 1, r) < \text{tol}$ :
             $\lambda_r = X^k(r, r)$ 
             $Q = Q \cdot \begin{bmatrix} Q_{\text{tmp}} & \mathbf{0} \\ \mathbf{0} & I_{n-r} \end{bmatrix}$ 
            break
     $\lambda_1 = X^k(1, 1)$ 
end
output:  $\lambda_i, i = 1, \dots, n; Q \in \mathbb{R}^{n \times n}$ 

```

## 5.2 Appendix-1.2: example of the output in part 1

In this example, the following matrix  $A$  is applied to the program.

$$A = \begin{bmatrix} 17 & 21 & 31 & 45 \\ 21 & 32 & 78 & 10 \\ 9 & 15 & 2 & 62 \\ 20 & 42 & 54 & 73 \\ 38 & 25 & 2 & 19 \\ 45 & 36 & 27 & 18 \end{bmatrix}$$

To verify whether the QR iteration or the alternative iterative procedure give a precise result, the python inbuilt function `numpy.linalg.svd` is used to compare with the output.

```
====using inbuilt function===
u = [[-0.3797757 -0.1378386 0.10061487 0.41164051 -0.5513195 -0.59434543]
      [-0.44557143 0.71238318 0.25918895 0.34791761 0.29961636 0.12641506]
      [-0.29879357 -0.62661455 0.09569395 0.474649 0.2040122 0.49194169]
      [-0.62136107 -0.19682153 0.30720626 -0.68235859 0.10056825 -0.0711955 ]
      [-0.22955482 -0.09289239 -0.66585362 0.06258666 0.56046581 -0.42104101]
      [-0.35940774 0.18302245 -0.61302829 -0.12117514 -0.49032639 0.45433665]]

s = [160.96588461 68.00857647 48.16852327 3.95106119]

v = [[-0.34681872 -0.45121064 -0.56435451 -0.59802151]
      [ 0.11391105 0.08953152 0.64943458 -0.74648718]
      [-0.80405037 -0.28376381 0.46156394 0.24482611]
      [ 0.46930166 -0.8413508 0.21609593 0.1587052 ]]
```

Figure 12: the SVD of  $A$  using python inbuilt function

```
====testing====
u = [[ 0.3797757 -0.1378386 -0.10061487 -0.41164051 0.5513195 -0.59434543]
      [ 0.44557143 0.71238318 -0.25918895 -0.34791761 -0.29961636 0.12641506]
      [ 0.29879357 -0.62661455 -0.09569395 -0.474649 -0.2040122 0.49194169]
      [ 0.62136107 -0.19682153 -0.30720626 0.68235859 -0.10056825 -0.0711955 ]
      [ 0.22955482 -0.09289239 0.66585362 -0.06258666 -0.56046581 -0.42104101]
      [ 0.35940774 0.18302245 0.61302829 0.12117514 0.49032639 0.45433665]]

s = [[160.96588461 0. 0. 0. ]
      [ 0. 68.00857647 0. 0. ]
      [ 0. 0. 48.16852327 0. ]
      [ 0. 0. 0. 3.95106119]
      [ 0. 0. 0. 0. ]
      [ 0. 0. 0. 0. ]]

v = [[ 0.34681872 0.45121064 0.56435451 0.59802151]
      [ 0.11391105 0.08953152 0.64943458 -0.74648718]
      [ 0.80405037 0.28376381 -0.46156394 -0.24482611]
      [-0.46930166 0.8413508 -0.21609593 -0.1587052 ]]

recover result: [[17. 24. 31. 45.]
                 [21. 32. 78. 10.]
                 [ 9. 15.  2. 62.]
                 [20. 42. 54. 73.]
                 [38. 25.  2. 19.]
                 [45. 36. 27. 18.]
```

Figure 13: the SVD of  $A$  using QR iteration with wilkinson shift and deflation



```

===using alternative iteration===
u = [[ 0.3797757  0.1378386 -0.10061487 -0.41164051 -0.5513195 -0.59434543]
      [ 0.44557143 -0.71238318 -0.25918895 -0.34791761  0.29961636  0.12641506]
      [ 0.29879357  0.62661455 -0.09569395 -0.474649  0.2040122  0.49194169]
      [ 0.62136107  0.19682153 -0.30720626  0.68235859  0.10056825 -0.0711955 ]
      [ 0.22955482  0.09289239  0.66585362 -0.06258666  0.56046581 -0.42104101]
      [ 0.35940774 -0.18302245  0.61302829  0.12117514 -0.49032639  0.45433665]]

s = [[160.96588461  0.  0.  0.  0.  0.]
      [ 0.  68.00857647  0.  0.  0.  0.]
      [ 0.  0.  48.16852327  0.  0.  0.]
      [ 0.  0.  0.  3.95106119  0.  0.]
      [ 0.  0.  0.  0.  0.  0.]
      [ 0.  0.  0.  0.  0.  0.]]

v = [[ 0.34681872  0.45121064  0.56435451  0.59802151]
      [-0.11391105 -0.08953152 -0.64943458  0.74648718]
      [ 0.80405037  0.28376381 -0.46156394 -0.24482611]
      [-0.46930166  0.8413508 -0.21609593 -0.1587052 ]]

recover result = [[17. 24. 31. 45.]
                  [21. 32. 78. 10.]
                  [ 9. 15.  2. 62.]
                  [20. 42. 54. 73.]
                  [38. 25.  2. 19.]
                  [45. 36. 27. 18.]]

```

Figure 14: the SVD of  $A$  using alternative iterative procedure

### 5.3 Appendix-2.1: examples and data obtained when measuring the quality of reconstruction in model I

\*  $256 \times 256$  images

image	trancation number	PSNR
256_256_hand.png	90	22.419
	95	23.049
	100	23.525
	101	23.701
	102	23.683
	105	20.068
256_256_buildings.png	90	19.972
	95	20.475
	101	21.016
	102	21.038
	103	21.056
	105	19.193

\*  $512 \times 512$  images

image	trancation number	PSNR
512_512_books.png	190	25.065
	195	25.278
	200	25.475
	204	25.629
	205	25.640
	206	25.639
	210	24.897
512_512_pens.png	190	29.613
	195	29.921
	200	30.148
	204	30.237
	205	30.311
	206	30.204
	210	27.112

\*  $1024 \times 1024$  images

image	trancation number	PSNR
1024_1024_stones.png	380	34.443
	390	34.698
	400	34.932
	409	34.978
	410	34.964
	420	30.124
	430	19.935
1024_1024_coffee.png	380	29.576
	390	29.827
	400	30.054
	405	30.131
	406	30.145
	407	30.137
	410	30.093
	420	25.506
	430	15.266

\* examples of blurring and deblurring an image using model I



(a) blurry image of 1024\_1024\_books.png



(b) reconstruct image of 1024\_1024\_books.png

**Figure 15:** blurry and reconstructed images of 1024\_1024\_books.png with  $l_{\text{trunc}} = r_{\text{trunc}} = 406$



(a) blurry image of 512\_512\_fruits.png



(b) reconstruct image of 512\_512\_fruits.png

**Figure 16:** blurry and reconstructed images of 512\_512\_fruits.png with  $l_{\text{trunc}} = r_{\text{trunc}} = 203$

## 5.4 Appendix-2.2: examples and data obtained when measuring the quality of reconstruction in model II

\* 256 \* 256 images

image	trancation number	PSNR
256_256_casino.png	235	15.281
	240	15.977
	245	19.716
	250	25.967
	255	34.852
	256	92.925
256_256_buildings.png	235	18.836
	240	22.203
	245	22.787
	250	28.612
	255	31.804
	256	144.035

\* 512 \* 512 images

image	trancation number	PSNR
512_512_car_01.png	490	22.692
	495	23.454
	500	25.096
	505	31.556
	510	33.206
	512	95.601
512_512_fruits.png	490	15.483
	495	21.727
	500	21.816
	505	23.228
	510	28.150
	512	117.785

\* examples of blurring and deblurring an image using model II



(a) blurry image of 1024\_1024\_coffee.png



(b) reconstruct image of 1024\_1024\_coffee.png

**Figure 17:** blurry and reconstructed images of 1024\_1024\_coffee.png with  $l_{\text{trunc}} = r_{\text{trunc}} = 1020$  (PSNR = 27.584)

### 5.5 Appendix-2.3: comparing performance of QR iteration with Wilkinson Shift and alternative iteration

\* QR iteration

image	run time	PSNR
256_256_hand.png	1.209	23.525
512_512_pens.png	13.696	30.311
640_640_lion.png	27.530	20.159

\* alternative iteration

image	run time	PSNR
256_256_hand.png	1.684	23.518
512_512_pens.png	20.011	30.313
640_640_lion.png	40.860	20.172

## 5.6 Appendix-3.1: More background extraction examples



**Figure 18:** 10 frames, 1 iteration



**Figure 19:** 10 frames, 3 iterations



**Figure 20:** 10 frames, 5 iterations

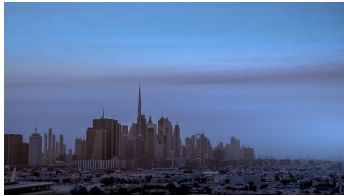


**Figure 21:** 20 frames, 3 iterations

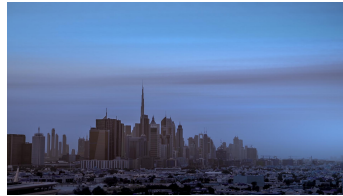


**Figure 22:** 50 frames, 3 iterations



**Figure 23:** 100 frames, 3 iterations



**Figure 24:** 10 frames, 1 iteration



**Figure 25:** 10 frames, 3 iterations



**Figure 26:** 10 frames, 5 iterations



**Figure 27:** 20 frames, 3 iterations



**Figure 28:** 50 frames, 3 iterations



**Figure 29:** 100 frames, 3 iterations